

Journal of Materials Chemistry A

Accepted Manuscript



This is an *Accepted Manuscript*, which has been through the Royal Society of Chemistry peer review process and has been accepted for publication.

Accepted Manuscripts are published online shortly after acceptance, before technical editing, formatting and proof reading. Using this free service, authors can make their results available to the community, in citable form, before we publish the edited article. We will replace this *Accepted Manuscript* with the edited and formatted *Advance Article* as soon as it is available.

You can find more information about *Accepted Manuscripts* in the [Information for Authors](#).

Please note that technical editing may introduce minor changes to the text and/or graphics, which may alter content. The journal's standard [Terms & Conditions](#) and the [Ethical guidelines](#) still apply. In no event shall the Royal Society of Chemistry be held responsible for any errors or omissions in this *Accepted Manuscript* or any consequences arising from the use of any information it contains.

COMMUNICATION

Hollow Carbon Spheres with Encapsulated Germanium as an Anode Material for Lithium Ion Batteries

Cite this: DOI: 10.1039/x0xx00000x

Received 00th January 2012,
Accepted 00th January 2012

DOI: 10.1039/x0xx00000x

www.rsc.org/

Dan Li,^{a,b} Chuanqi Feng,^a Hua kun Liu,^b Zaiping Guo^{*a,b,c}

A novel composite consisting of hollow carbon spheres with encapsulated germanium (Ge@HCS) was synthesized by introducing germanium precursor into the porous-structured hollow carbon spheres. The carbon spheres not only function as a scaffold to hold the germanium and thus maintain the structural integrity of the composite, but also increase the electrical conductivity. The voids and vacancies that are formed after the reduction of germanium dioxide to germanium provide free space for accommodating the volume changes during discharging/charging processes, thus preventing pulverization. The obtained Ge@HCS composite exhibits excellent lithium storage performance, as revealed by electrochemical evaluation.

Introduction

The increasing demand for clean and green energy is currently shifting towards alternative energy sources such as wind power, tidal power, solar cells, fuel cells, and batteries.¹ Lithium ion batteries have been considered to be the most promising energy storage system for portable electrical devices, electric vehicles, hybrid electric vehicles, etc.² Lithium ion batteries are more suitable for such purposes compared to previous conventional batteries, including metal hydride, alkaline, and lead-acid batteries, due to their high power density and high energy density. To further satisfy the demand, much research has been recently focused on high capacity materials. Group IVA materials have attracted significant interest as anode materials for lithium ion batteries due to their high theoretical capacity, especially silicon and germanium, which exhibit high theoretical capacities of 4200 mA h g⁻¹ and 1623 mA h g⁻¹ (4.4 Li⁺ per silicon or germanium atom), respectively.³⁻⁶ In the case of silicon, its practical use in commercial application is limited by inferior cycling performance because of the great volume changes

during cycling and the poor rate capability caused by its inherent low ionic diffusivity and electronic conductivity. Compared to silicon, germanium can boost the electrical conductivity to two orders of magnitude higher, and the lithium diffusivity to four orders of magnitude faster.^{3, 7} Furthermore, it has been proved that the total system energy can be dramatically decreased by the high adsorption energy of lithium ions on the germanium surface.⁵ These outstanding properties make germanium an excellent candidate anode material for lithium ion batteries. Like silicon, however, the major drawback of germanium is the large volume change during lithiation/delithiation processes, which results in cracking, pulverization, and loss of electrode contact, leading to poor cyclability and capacity fading.⁸ Synthesis of nanostructured morphologies, such as nanofiber,⁹ nanowires,^{4, 8, 10-12} nanotubes,^{5, 13} and nanoparticles,¹⁴ is an effective method to address this issue by accommodating the volume change, introducing relaxation mechanisms to tolerate strain, and alleviating the pulverization. Another significant strategy is developing a carbon-based germanium composite that not only provides a volume expansion buffer for lithium ion intercalation, but also improves the electrical conductivity of the material. There are many previous studies that have reported germanium modified by various carbon sources, for example, nanostructured germanium interconnected by carbon synthesized by a reduction reaction between amorphous GeO₂ and carbon,¹⁵ single crystalline germanium nanowires sheathed with carbon prepared by a solid-liquid solution method,⁴ self-assembled germanium-carbon nanostructures obtained through carbon coating and reduction of the oxide precursor,¹⁴ carbon covered germanium particles embedded into reduced graphene oxide networks,¹⁶ sandwich-structured C/Ge/graphene composite synthesized by a microwave-assisted solvothermal reaction and then carbon-coating the surface of the germanium/graphene precursor.¹⁷ Hollow carbon spheres (HCS) have attracted considerable attention because of their promising applications in catalysis, lithium-ion batteries, fuel cells, supercapacitors, and water treatment.^{18, 19} Resorcinol-formaldehyde

resin (RF) is considered as one of the most fascinating and versatile carbon precursors for the designed synthesis of HCS.²⁰ Moreover, it is reported that cetyl trimethyl ammonium bromide (CTAB) modified HCS are endowed with a uniform microporous structure with superior surface properties, which could be beneficial to the introduction of metal precursors. Therefore, their unique structure makes HCS a good candidate for synthesizing a composite with germanium encapsulated in carbon spheres.

Herein, hollow carbon spheres were firstly synthesized using silicon spheres as hard templates. The carbon spheres were modified by CTAB in the process of RF coating to obtain a porous structure, which not only increases the contact area between the electrode and electrolyte, but also facilitates the introduction of the germanium precursor. Within this architecture, the germanium can freely undergo lithiation/de-lithiation processes without agglomeration due to the protecting scaffold effect of the carbon spheres and the voids that are formed after the reduction treatment of the precursor, thus securing the structural and electrical integrity of the electrode during repeated cycling. This unique encapsulation of germanium in hollow carbon spheres endows the obtained materials with enhanced electrochemical properties.

Results and discussion

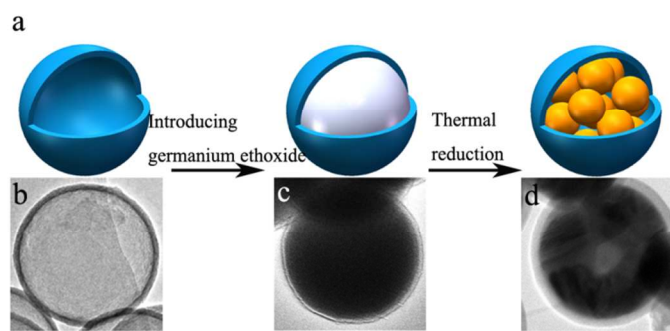


Fig. 1. (a) Schematic illustration of the formation process to incorporate the germanium in the hollow carbon spheres. TEM images of (b) HCS, (c) GeO_2 @HCS, and (d) Ge @HCS.

Fig. 1 illustrates the general route to synthesize the Ge @HCS composite through introducing germanium ethoxide into the hollow carbon spheres, followed by a thermal reduction treatment. In a typical synthetic procedure, the SiO_2 template spheres are synthesized by a modified Stöber method and then covered with a uniform carbon layer transformed from carbonization of the self-assembled RF and CTAB. After etching with NaOH, the hollow carbon spheres are formed. It is noteworthy that the participation of the cationic surfactant CTAB plays a significant role in the surface properties of the silica templates. The cationic CTAB can decorate the spheres with positive charges by forming a bi-layer structure, which can easily make the negatively charged RF form a coating on the negatively charged Stöber silica spheres,²¹ promoting the following self-assembly of CTAB and RF on the silica sphere surfaces to form a polymer shell. Importantly, the CTAB modified polymer shells can be transformed to uniform microporous carbon spheres because of the elimination of CTAB after the carbonization treatment.²² Therefore, the structure features carbon spheres equipped with high dispersibility and discreteness,²³ which can have an affinity with the germanium ethoxide and thus allow it to

penetrate the carbon layer and go into the center of a hollow carbon sphere under vacuum conditions. After a long stirring over 2 days, the vacuum beaker is gradually filled with air to ensure that the germanium ethoxide is hydrolyzed to $\text{Ge}(\text{OH})_4$ and then converted to GeO_2 . The obtained GeO_2 @HCS undergoes a thermal reduction treatment and is finally transformed to Ge @HCS.

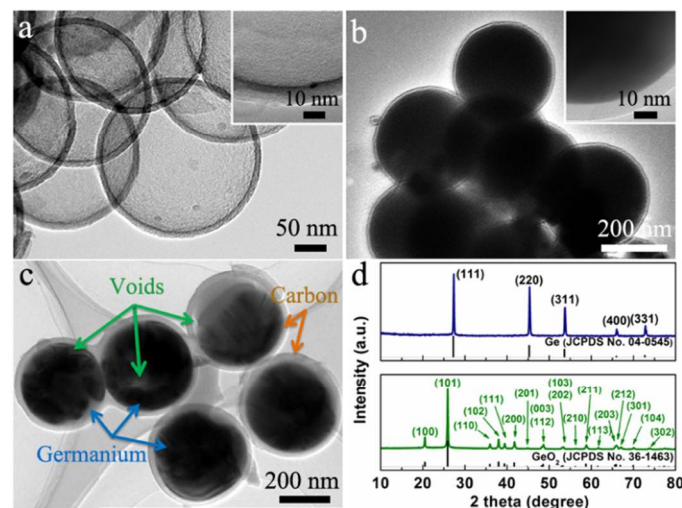


Fig. 2. TEM images of (a) HCS, (b) GeO_2 @HCS, and (c) Ge @HCS. (d) Powder X-ray diffraction patterns of the obtained GeO_2 @HCS and Ge @HCS samples.

Fig. S1 and Fig. 1(a) contain SEM images of the SiO_2 templates, which consist of relatively monodisperse nanospheres about 250 nm in size. After the coating with RF resin and the following carbonization treatment, the hollow carbon spheres were obtained, which kept their uniform and monodisperse structure, as can be observed in the SEM and TEM images in Fig. S2. Germanium ethoxide was introduced into the carbon spheres under vacuum and converted to GeO_2 after a long stirring process to facilitate a complete hydrolysis and oxidation reaction. The vacuum strategy is effective for loading the germanium precursor, which can be proved from the TEM image shown in Fig. 2(b), indicating that the hollow centers of the HCS were fully occupied by GeO_2 . SEM images of GeO_2 @HCS are shown in Fig. S3. After completion of the thermal reduction process, relatively thinner areas appeared inside the carbon spheres, which were stems from the produced voids and pores due to the release of oxygen when GeO_2 was reduced to elemental germanium (See Fig. 2(c)). From the SEM images (as shown in Fig. S4), it can be found from broken carbon spheres that there are germanium particles inside the carbon spheres. Energy dispersive X-ray spectroscopy (EDS) gives further evidence to confirm the presence of germanium in the Ge @HCS sample in Fig. S5. On the other hand, GeO_2 @C particles were synthesized for comparison by natural hydrolysis of the germanium ethoxide precursor without the presence of HCS under the identical synthesis conditions as those for the GeO_2 @HCS sample. The as-prepared GeO_2 bulks (shown in Fig. S6) were transformed to GeO_2 /C bulks after the carbon-coating treatment, and then were further transformed to Ge @C particles after the thermal reduction process. Images of the morphology of the GeO_2 /C bulks and Ge @C particles are shown in Fig. S7 and S8, respectively. X-ray diffraction (XRD) was applied to characterize the crystal structures of the obtained GeO_2 @HCS and Ge @HCS samples, as shown in Fig. 2(d). All the reflection peaks of the GeO_2 @HCS are well indexed to the hexagonal phase of GeO_2 (JCPDS card No. 36-1463). After the reduction treatment, the

hexagonal phase is converted to diamond cubic phase (Ge) (JCPDS card No. 40-0545). There are no peaks corresponding to carbon that can be detected in the pattern, which could be attributed to their overlapping with the (111) peak of germanium at around 27°.

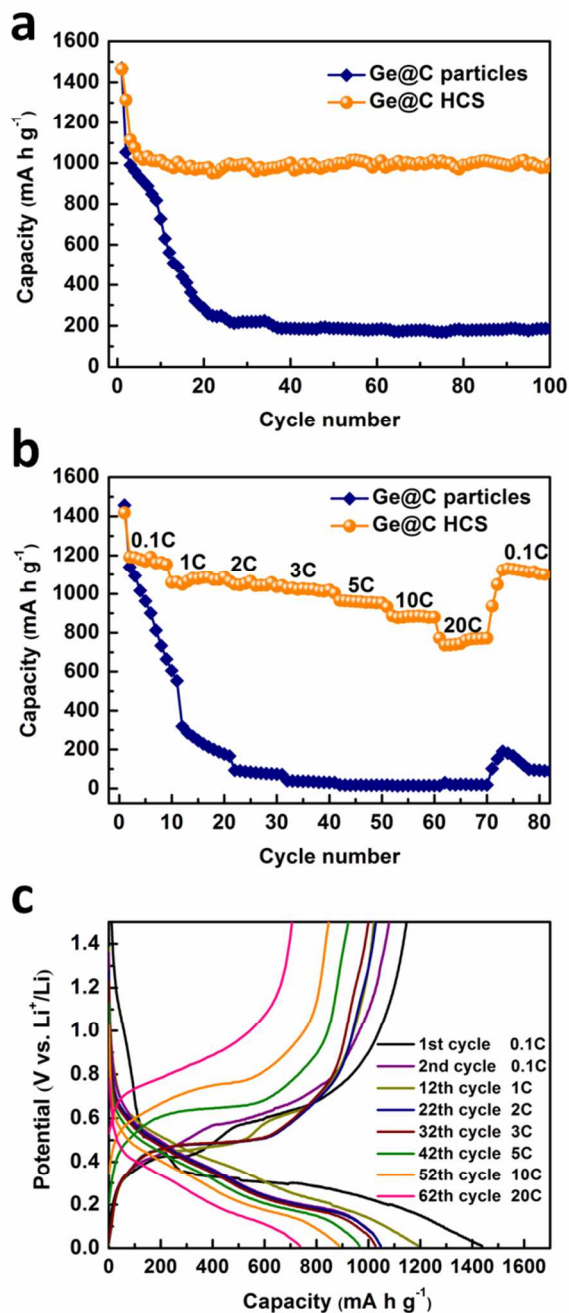


Fig. 3. (a) Cycling performance of the Ge@C particles and the Ge@HCS sample at 0.4 C current rate over 100 cycles. (b) Comparison of rate capability of Ge@C particles and Ge@HCS sample at different current densities (charging rates from 0.1–20 C, with discharge at 0.2 C). (c) Galvanostatic charge–discharge profiles of the Ge@HCS composite at different current densities from 0.1–20 C (corresponding to (b)).

The carbon content of the Ge@C particles and Ge@HCS composites was investigated by thermogravimetric analysis (TGA), and the

calculated values are 11.9 wt% and 10.3 wt%, respectively, as shown in Fig. S9. Raman spectroscopy, as shown in Fig. S10, was applied to analyze the chemical bonding in the composites due to its high sensitivity to electronic structure. The peak at 294 cm^{-1} is attributed to the optical mode of crystalline germanium. Moreover, there is a strong D band at 1345 cm^{-1} related to the presence of defects, as well as a G band at 1605 cm^{-1} that is ascribed to the E_{2g} vibrational mode for the sp^2 domain.²⁴

The hollow carbon spheres encapsulating germanium with structural stability can offer excellent lithium storage performance, and the results are shown in Fig. 3. For comparison, the cycling performances of Ge@C particles and Ge@HCS electrode are exhibited in Fig. 3(a) up to 100 cycles at the rate of 0.4 C. The current density for the 1 C rate is 1600 mA g^{-1} . The Ge@HCS electrode delivers a significantly high specific capacity of about 1455 mA h g^{-1} at the first cycle, corresponding to the quite high specific capacity of 1617 mA h g^{-1} for germanium alone, which is very close to the theoretical capacity of germanium. The capacity remains almost constant after the fifth cycle. On the other hand, it can be observed that the Ge@C particle electrode shows very fast capacity fading with only a negligible specific capacity value of 185 mA h g^{-1} at the 100th cycle. The rate capability of the Ge@HCS electrode was evaluated at various current rates, and the obtained results are shown in Fig. 3(b) (charging at 0.1–20 C and discharging at 0.2 C). The Ge@HCS shows much enhanced rate performance compared to the Ge@C particle sample at all current rates. There was a negligible capacity drop when the charging current was increased from 1 C to 3 C. The discharge capacity was 1153.3 mA h g^{-1} at the 10th cycle at the rate of 0.1 C, 953 mA h g^{-1} at the 50th cycle at 5 C, and 878.9 mA h g^{-1} at the 60th cycle at the rate of 10 C. Even at the high rate of 20 C, the specific capacity remained 772.5 mA h g^{-1} , which is still 67% of its capacity at 0.1 C. Subsequently, the rate went back to 0.1 C, at which the specific capacity reached a value of 1140 mA h g^{-1} and therefore almost recovered, indicating excellent reversibility. In contrast, a low capacity of only 20 mA h g^{-1} was obtained from the Ge@C particle sample at the rate of 20 C. The poor capacity recovery of the Ge@C particles is probably due to the pulverization of germanium particles induced by the unavoidable volume changes during the lithium ion insertion/extraction processes, leading to the loss of electrical contact. Fig. 3(c) shows the galvanostatic voltage profiles of the Ge@HCS composite electrode in the 1st, 2nd, 12nd, 22nd, 32nd, 42nd, 52nd, and 62nd cycles at different rates, showing that all lithium ion insertion and extraction processes are spread over a relatively broad voltage range, and therefore, are also separated temporally. Fig. S11 are the SEM images of Ge@HCS composite electrode after cycling (100 cycles), indicating that the hollow carbon spheres are robust enough to remain the structural stability.

The much improved cycling stability and rate capability of the Ge@HCS sample may be ascribed to the distinct structure and morphology, which offer the following benefits. Firstly, the hollow carbon spheres can function as a physical matrix to effectively prevent the germanium cores from coalescing into a bulk during lithiation/de-lithiation processes, and also protect the germanium cores against pulverization. Secondly, the germanium cores are interconnected by the shells of the carbon spheres, forming an effective and continuous conductive network to significantly facilitate the diffusion and transport of lithium ions even at high current rates. Thirdly, the inherently porous nature of Ge@HCS with many voids can ensure a high contact area between the electrolyte and electrode materials, and thus facilitate the transport and diffusion of lithium ions. More importantly, the porous property can endow the composite with free space to accommodate the volume changes

in the germanium during the charging/discharging processes, thus maintaining the structural integrity of the electrode.

Conclusions

In summary, a novel composite consisting of hollow carbon spheres with encapsulated germanium was first synthesized through infiltrating the germanium precursor into the carbon spheres, which were obtained by carbonization of a CTAB modified RF resin coating on silicon template spheres, followed by etching the templates. The cationic surfactant CTAB served as a soft template for mesostructured RF resin formation, resulting in a porous carbon shell, which facilitates the access of the germanium precursor to its hollow center. The obtained Ge@HCS material shows excellent electrochemical properties, which can be attributed to the unique morphology and structure. The voids and vacancies that are formed after the shrinkage of GeO₂ to form germanium can effectively accommodate the volume changes during the lithiation/de-lithiation processes, enabling structural integrity and continuity. Meanwhile, the carbon spheres can serve as a network of electronic pathways, which could increase the kinetics of lithium reactions. The strategy of encapsulating germanium in HCS could offer a new method for developing anode electrodes with high performance.

Acknowledgements

This work was partially supported by the National Natural Science Foundation of China (21476063), and the Australian Research Council through a Discovery Project (DP1094261). Part of this research was undertaken at Prof. Xiongwen Lou's laboratory at Nanyang Technological University, and the authors acknowledge the great support that they received from Prof. Xiongwen Lou. The authors also would like to thank Dr. Tania Silver for critical reading of the manuscript.

Notes and references

^a Hubei Collaborative Innovation Center for Advanced Organic Chemical Materials, College of Chemistry and Chemical Engineering, Hubei University, Wuhan 430062, China.

^b Institute for Superconducting and Electronic Materials, University of Wollongong, Wollongong, NSW 2522, Australia.

^c School of Mechanical, Materials and Mechatronics Engineering, University of Wollongong, North Wollongong, NSW 2500, Australia.

Electronic Supplementary Information (ESI) available: [details of any supplementary information available should be included here]. See DOI: 10.1039/c000000x/

1. C.-M. Park, J.-H. Kim, H. Kim and H.-J. Sohn, *Chem. Soc. Rev.*, 2010, **39**, 3115.
2. L. Ji, Z. Lin, M. Alcoutlabi and X. Zhang, *Energy Environ. Sci.*, 2011, **4**, 2682.
3. H. Lee and J. Cho, *Nano Lett.*, 2007, **7**, 2638.
4. M.-H. Seo, M. Park, K. T. Lee, K. Kim, J. Kim and J. Cho, *Energy Environ. Sci.*, 2011, **4**, 425.
5. T. Song, H. Cheng, H. Choi, J.-H. Lee, H. Han, D. H. Lee, D. S. Yoo, M.-S. Kwon, J.-M. Choi, S. G. Doo, H. Chang, J. Xiao, Y. Huang, W. I. Park, Y.-C. Chung, H. Kim, J. A. Rogers and U. Paik, *ACS Nano*, 2011, **6**, 303.
6. Y. Yu, C. Yan, L. Gu, X. Lang, K. Tang, L. Zhang, Y. Hou, Z. Wang, M. W. Chen, O. G. Schmidt and J. Maier, *Adv. Energy Mater.*, 2013, **3**, 281.
7. J. Graetz, C. C. Ahn, R. Yazami and B. Fultz, *J. Electrochem. Soc.*, 2004, **151**, A698.
8. F.-W. Yuan, H.-J. Yang and H.-Y. Tuan, *ACS Nano*, 2012, **6**, 9932.
9. W. Li, Z. Yang, J. Cheng, X. Zhong, L. Gu and Y. Yu, *Nanoscale*, 2014, **6**, 4532.
10. C. K. Chan, X. F. Zhang and Y. Cui, *Nano Lett.*, 2007, **8**, 307.
11. X. H. Liu, S. Huang, S. T. Picraux, J. Li, T. Zhu and J. Y. Huang, *Nano Lett.*, 2011, **11**, 3991.
12. J. Liu, K. Song, C. Zhu, C.-C. Chen, P. A. van Aken, J. Maier and Y. Yu, *ACS Nano*, 2014, **8**, 7051.
13. M.-H. Park, Y. Cho, K. Kim, J. Kim, M. Liu and J. Cho, *Angew. Chem. Int. Ed.*, 2011, **50**, 9647.
14. K. H. Seng, M.-H. Park, Z. P. Guo, H. K. Liu and J. Cho, *Angew. Chem. Int. Ed.*, 2012, **51**, 5657.
15. D. T. Ngo, R. S. Kalubarme, H. T. T. Le, J. G. Fisher, C.-N. Park, I.-D. Kim and C.-J. Park, *Adv. Funct. Mater.*, 2014, **24**, 5291.
16. D.-J. Xue, S. Xin, Y. Yan, K.-C. Jiang, Y.-X. Yin, Y.-G. Guo and L.-J. Wan, *J. Am. Chem. Soc.*, 2012, **134**, 2512.
17. D. Li, K. H. Seng, D. Shi, Z. Chen, H. K. Liu and Z. Guo, *J. Mater. Chem. A*, 2013, **1**, 14115.
18. K. T. Lee, Y. S. Jung and S. M. Oh, *J. Am. Chem. Soc.*, 2003, **125**, 5652.
19. W.-M. Zhang, J.-S. Hu, Y.-G. Guo, S.-F. Zheng, L.-S. Zhong, W.-G. Song and L.-J. Wan, *Adv. Mater.*, 2008, **20**, 1160.
20. F. Zhang, Y. Meng, D. Gu, Yan, C. Yu, B. Tu and D. Zhao, *J. Am. Chem. Soc.*, 2005, **127**, 13508.
21. N. Li, Q. Zhang, J. Liu, J. Joo, A. Lee, Y. Gan and Y. Yin, *Chem. Commun.*, 2013, **49**, 5135.
22. N. Nishiyama, T. Zheng, Y. Yamane, Y. Egashira and K. Ueyama, *Carbon*, 2005, **43**, 269.
23. X. Fang, J. Zang, X. Wang, M.-S. Zheng and N. Zheng, *J. Mater. Chem. A*, 2014, **2**, 6191.
24. J. Shen, Y. Hu, M. Shi, X. Lu, C. Qin, C. Li and M. Ye, *Chem. Mater.*, 2009, **21**, 3514.

